

Mixed halide hybrid halobismuthates and their *in situ* transformations

Vitalii Yu. Kotov, Andrey B. Ilyukhin, Petr A. Buikin and Khursand E. Yorov

Table of contents

Synthesis of compounds 1a–4f	S1
Tables S1–S5 Results of EDX analyses for 1b–4b and 4f	S3
Table S6 Crystal data and structure refinement for 1b–4d	S4
Table S7 Bond lengths [Å] in compounds 1b–4d	S6
Figure S1 X-ray Rietveld refinement profiles for 1b–4b	S11
Figure S2 The reflectance spectra of 1b–4b and 4c	S12
Figure S3 ¹ H NMR spectra of 1a–4a	S13
Figures S4–S11 Additional structural data for compounds 1b–4e	S15
Figure S12 XRD patterns for compounds 4f , 4e , and 4d	S23

Synthesis of compounds 1a–3a. CHI (27.8 g, 196 mmol) was added to a solution of the corresponding picoline (14.9 g, 160 mmol) in 96% ethanol (25 ml), and the mixture was kept for one day in a closed flask at room temperature. The resulting beige precipitate was filtered off *in vacuo* and dried in the air. The yields were for **1a**: 29.72 g (79.0%) and for **3a**: 28.82 g (76.6%). Product **2a** was a highly hygroscopic compound, which we failed to isolate in a dry form. The nature and purity of the obtained products were confirmed by ¹H NMR (300 MHz, D₂O, Figure S3(a–c)). ¹H NMR data for **1a**: 8.60 (d, 1H), 8.27 (t, 1H), 7.80 (m, 1H), 7.73 (m, 1H), 4.14 (s, 3H), 2.70 (s, 3H). ¹H NMR data for **2a**: 8.55 (s, 1H), 8.49 (d, 1H), 8.25 (d, 1H), 7.81 (t, 1H), 4.24 (s, 3H), 2.44 (s, 3H). ¹H NMR data for **3a**: 8.47 (d, 2H), 7.75 (d, 2H), 4.20 (s, 3H), 2.54 (s, 3H).

Synthesis of compounds 1b–3b. A solution of Bi(NO₃)₃·5H₂O (1.03 g, 2.1 mmol) and KBr (4.48 g, 37.6 mmol) in H₂O (10 ml) was added to an aqueous solution containing corresponding iodide **1a** or **3a** (0.50 g, 2.1 mmol), KBr (2.24 g, 18.8 mmol), and H₂O (10 ml). The yellowish-orange crystalline precipitate was formed and kept in the mother liquor at room temperature.

After two days, the resulting precipitate was filtered off *in vacuo* and dried in the air. The yields were for **1b**: 0.696 g (10.5%) and for **3b**: 0.766 g (23.1%). The reaction of **2a** was carried out in a similar way using 1 g of the wet compound instead of 0.5 g of the dry compound as was in the cases of **1a** and **3a**. Yield: 1.398 g.

Synthesis of compound 3c. A solution of $\text{Bi}(\text{NO}_3)_3 \cdot 5\text{H}_2\text{O}$ (1.03 g, 2.1 mmol) and KI (6.25 g, 37.7 mmol) in H_2O (10 ml) was added to an aqueous solution containing iodide **3a** (0.50 g, 2.1 mmol), KI (3.12 g, 18.8 mmol), and H_2O (10 ml), and the formed red fine-crystalline precipitate was kept in the mother liquor at room temperature. After two days, the precipitate was filtered off *in vacuo* and dried in the air. The yield was 1.33 g (76.8%).

Synthesis of compound 4a. CH_3I (22.7 g, 160 mmol) was added to a solution of 4-cyanopyridine (16.6 g, 160 mmol) in 96% ethanol (25 ml), and the mixture was kept for one day in a closed flask at room temperature. The resulting yellowish-orange precipitate of **4a** was filtered off *in vacuo* and dried in the air. The yield was 12.21 g (31.0%). The nature and purity of the product obtained were confirmed by ^1H NMR (300 MHz, D_2O , Figure S3(d)): 9.01 (d, 2H), 8.38 (d, 2H), 4.40 (s, 3H).

Synthesis of compound 4b. A solution of $\text{Bi}(\text{NO}_3)_3 \cdot 5\text{H}_2\text{O}$ (0.985 g, 2.0 mmol) and KBr (4.28 g, 36.0 mmol) in H_2O (10 ml) was added to an aqueous solution containing iodide **4a** (0.50 g, 2.0 mmol), KBr (2.14 g, 18.0 mmol), and H_2O (10 ml). The orange crystalline precipitate was formed and kept in the mother liquor at room temperature. After two days, orange crystals of **4b** were filtered off *in vacuo* and dried in the air. The yield was 0.625 g (17.3%).

Synthesis of compound 4f. A solution of $\text{Bi}(\text{NO}_3)_3 \cdot 5\text{H}_2\text{O}$ (0.985 g, 2.0 mmol) and KI (6.00 g, 36.1 mmol) in H_2O (10 ml) was added to an aqueous solution containing iodide **4a** (0.50 g, 2.0 mmol), KI (3.00 g, 18.1 mmol), and H_2O (10 ml). The red precipitate was formed and kept in the mother liquor at room temperature. After two days, the resulting precipitate of **4f** was filtered off *in vacuo* and dried in the air. The yield was 1.138 g.

Table S1 Results of EDX analysis (at%) for compound **1b** normalized with respect to Bi.

Spectrum	Bi	Br	I	Br/Hal (%) ^a
Spectrum 1	1	3.31	1.28	72.1
Spectrum 2	1	3.28	1.33	71.1
Spectrum 3 (overview)	1	3.53	1.23	74.2

^a The halogen ratio Br/Hal in initial solution (before precipitation) was 96.4%

Table S2 Results of EDX analysis (at%) for compound **2b** normalized with respect to Bi.

Spectrum	Bi	Br	I	Br/Hal (%)
Spectrum 1	1	3.20	1.34	70.5
Spectrum 2	1	3.15	1.31	70.6
Spectrum 3 (overview)	1	3.32	1.42	70.0

Table S3 Results of EDX analysis (at%) for compound **3b** normalized with respect to Bi.

Spectrum	Bi	Br	I	Br/Hal (%) ^a
Spectrum 1	1	3.46	1.03	77.1
Spectrum 2	1	3.07	1.33	69.8
Spectrum 3 (overview)	1	3.24	1.08	75.0

^a The halogen ratio Br/Hal in initial solution (before precipitation) was 96.4%

Table S4 Results of EDX analysis (at%) for compound **4b** normalized with respect to Bi.

Spectrum	Bi	Br	I	Br/Hal (%)
Spectrum 1	1	3.65	1.39	72.4
Spectrum 2	1	4.09	1.06	79.4
Spectrum 3	1	3.91	1.14	77.4
Spectrum 4 (overview)	1	3.83	1.28	75.0

^a The halogen ratio Br/Hal in initial solution (before precipitation) is 96.4%

Table S5 Results of EDX analysis (at%) for compound **4f** normalized with respect to Bi.

Spectrum	Bi	I	K
Spectrum 1	1	4.09	0.00
Spectrum 2	1	5.87	0.02
Spectrum 2	1	3.95	0.00
Spectrum 3 (overview)	1	4.64	0.06

Table S6 Crystal data and structure refinement parameters for compounds **1b–4e**.

Compound number ^a	1b	2b	3b	4b_100K	4b_150K
Empirical formula	C ₄₂ H ₆₀ Bi ₄ Br _{12.86} I _{5.14} N ₆	C ₂₁ H ₃₀ Bi ₂ Br _{6.26} I _{2.74} N ₃	C ₂₁ H ₃₀ Bi ₂ Br _{6.60} I _{2.40} N ₃	C ₂₈ H ₂₈ Bi ₂ Br _{7.42} I _{2.58} N ₈	C ₂₈ H ₂₈ Bi ₂ Br _{7.52} I _{2.48} N ₈
Formula weight	3164.79	1590.38	1574.40	1814.88	1810.18
<i>T</i> /K	150(2)	150(2)	150(2)	100(2)	150(2)
λ /Å	0.67522	0.71073	0.67522	0.71073	0.71073
Crystal system	Orthorhombic	Monoclinic	Monoclinic	Orthorhombic	Orthorhombic
Space group	<i>P</i> 2 ₁ 2 ₁ 2 ₁	<i>P</i> 2 ₁	<i>P</i> 2 ₁ / <i>n</i>	<i>P</i> bca	<i>P</i> bca
<i>a</i> /Å	10.2477(3)	11.8243(4)	18.7476(7)	16.7680(5)	16.8149(6)
<i>b</i> /Å	16.8771(3)	11.8539(4)	11.7296(3)	9.8073(3)	9.8623(4)
<i>c</i> /Å	42.4017(9)	13.3778(4)	19.0123(7)	27.5212(7)	27.5955(10)
β /deg	90	95.8019(11)	118.158(5)	90	90
<i>V</i> /Å ³	7333.4(3)	1865.48(11)	3686.0(3)	4525.8(2)	4576.3(3)
<i>Z</i>	4	2	4	4	4
<i>d</i> _{calc} /mg m ⁻³	2.866	2.831	2.837	2.664	2.627
μ /mm ⁻¹	16.382	18.408	16.335	16.107	15.949
<i>F</i> (000)	5634	1415	2805	3258	3251
Crystal size/mm	0.04 × 0.02 × 0.02	0.18 × 0.12 × 0.10	0.02 × 0.01 × 0.01	0.28 × 0.2 × 0.12	0.22 × 0.12 × 0.06
θ range/deg	1.465, 26.753	2.192, 30.052	1.994, 23.697	2.429, 28.315	2.422, 27.156
Index ranges	-10 ≤ <i>h</i> ≤ 10 -22 ≤ <i>k</i> ≤ 22 -56 ≤ <i>l</i> ≤ 56	-16 ≤ <i>h</i> ≤ 16 -16 ≤ <i>k</i> ≤ 16 -18 ≤ <i>l</i> ≤ 18	-22 ≤ <i>h</i> ≤ 22 -13 ≤ <i>k</i> ≤ 13 -22 ≤ <i>l</i> ≤ 22	-22 ≤ <i>h</i> ≤ 22 -13 ≤ <i>k</i> ≤ 13 -36 ≤ <i>l</i> ≤ 36	-21 ≤ <i>h</i> ≤ 21 -12 ≤ <i>k</i> ≤ 12 -35 ≤ <i>l</i> ≤ 35
Reflections collected	52603	64774	19649	53397	51753
Independent reflections, <i>R</i> _{int}	16331, 0.0412	10938, 0.0411	6245, 0.0344	5623, 0.0759	5076, 0.0782
Completeness to $\theta = 25.242^\circ$	94.2 %	99.9 %	95.9 %	100.0 %	100.0 %
Absorption correction	Semi-empirical from equivalents	Semi-empirical from equivalents	Semi-empirical from equivalents	Semi-empirical from equivalents	Semi-empirical from equivalents
Max., min. transmission	1, 0.73988	0.0232, 0.0026	1, 0.8548	0.2627, 0.0977	0.0943, 0.0258
Refinement method	Full-matrix least-squares on <i>F</i> ²	Full-matrix least-squares on <i>F</i> ²	Full-matrix least-squares on <i>F</i> ²	Full-matrix least-squares on <i>F</i> ²	Full-matrix least-squares on <i>F</i> ²
Data / restraints / parameters	16331 / 54 / 695	10938 / 1 / 367	6245 / 108 / 379	5623 / 0 / 226	5076 / 0 / 217
Goodness-of-fit	1.049	1.198	0.945	1.007	1.060
<i>R</i> ₁ , <i>wR</i> ₂ [<i>I</i> > 2 σ (<i>I</i>)]	0.0348, 0.0881	0.0450, 0.1108	0.0289, 0.0825	0.0353, 0.0788	0.0398, 0.0858
<i>R</i> ₁ , <i>wR</i> ₂ (all data)	0.0384, 0.0897	0.0490, 0.1128	0.0327, 0.0848	0.0552, 0.0866	0.0644, 0.0953
Absolute structure parameter	0.011(3)	-0.027(2)			
Largest diff. peak and hole/e.Å ⁻³	2.026, -1.349	2.386, -1.198	1.266, -1.070	1.882, -1.386	1.399, -1.460

	3c	4c	4d
Compound number	3c	4c	4d
Empirical formula	C ₇ H ₁₀ Bi ₄ N	C ₅₆ H ₅₆ Bi ₃ Br ₁₂ I ₁₅ N ₁₆	C ₃₅ H ₃₅ Bi ₂ I ₁₂ KN ₁₀
Formula weight	824.74	4442.52	2575.59
<i>T</i> /K	100(2)	150(2)	150(2)
λ /Å	0.71073	0.71073	0.71073
Crystal system	Monoclinic	Tetragonal	Monoclinic
Space group	<i>P</i> 2 ₁ / <i>c</i>	<i>I</i> 4/ <i>m</i>	<i>P</i> 2 ₁ / <i>n</i>
<i>a</i> /Å	14.4469(10)	14.7016(6)	9.8150(2)
<i>b</i> /Å	14.0102(10)	14.7016(6)	14.9572(3)
<i>c</i> /Å	7.7784(5)	24.3159(10)	20.8682(4)
β /deg	104.175(2)	90	92.0850(10)
<i>V</i> /Å ³	1526.44(18)	5255.6(5)	3061.53(11)
<i>Z</i>	4	2	2
<i>d</i> _{calc} /mg m ⁻³	3.589	2.807	2.794
μ /mm ⁻¹	19.608	14.017	11.891
<i>F</i> (000)	1416	3936	2272
Crystal size/mm	0.28 × 0.12 × 0.1	0.22 × 0.12 × 0.06	0.2 × 0.16 × 0.1
θ range/deg	2.908, 26.373	2.578, 31.023	2.262, 31.552
Index ranges	-18 ≤ <i>h</i> ≤ 18 -17 ≤ <i>k</i> ≤ 17 -9 ≤ <i>l</i> ≤ 9	-21 ≤ <i>h</i> ≤ 20 -20 ≤ <i>k</i> ≤ 20 -34 ≤ <i>l</i> ≤ 34	-14 ≤ <i>h</i> ≤ 14 -21 ≤ <i>k</i> ≤ 21 -30 ≤ <i>l</i> ≤ 30
Reflections collected	15899	37819	72867
Independent reflections, <i>R</i> _{int}	3116, 0.0387	4258, 0.0553	10022, 0.0631
Completeness to $\theta = 25.242^\circ$	99.8 %	99.9 %	100.0 %
Absorption correction	Semi-empirical from equivalents	Semi-empirical from equivalents	Semi-empirical from equivalents
Max., min. transmission	0.0473, 0.0093	0.0518, 0.0136	0.1015, 0.0255
Refinement method	Full-matrix least-squares on <i>F</i> ²	Full-matrix least-squares on <i>F</i> ²	Full-matrix least-squares on <i>F</i> ²
Data / restraints / parameters	3116 / 0 / 121	4258 / 0 / 149	10022 / 20 / 313
Goodness-of-fit	1.326	1.010	0.925
<i>R</i> ₁ , <i>wR</i> ₂ [<i>I</i> > 2 σ (<i>I</i>)]	0.0284, 0.0614	0.0339, 0.0904	0.0309, 0.0743
<i>R</i> ₁ , <i>wR</i> ₂ (all data)	0.0294, 0.0616	0.0549, 0.1003	0.0495, 0.0838
Largest diff. peak and hole/e.Å ⁻³	2.346, -1.167	1.665, -1.235	2.136, -0.982

^a **1b** = [1,2-Me₂Py]₆[Bi₂Br₆I₃][Bi₂Br_{6.85}I_{2.15}]; **2b** = [1,3-Me₂Py]₃[Bi₂Br_{6.26}I_{2.74}]; **3b** = [1,4-Me₂Py]₃[Bi₂Br_{6.60}I_{2.40}]; **4b** = [4-CNMePy]₄[Bi₂Br_{7.52}I_{2.48}];
3c = [1,4-Me₂Py][BiI₄]; **4c** = [4-CNMePy]₈[Bi₃Br₁₂I₄][I₇]·2(I₂); **4d** = [4-CNMePy]₅[K(BiI₆)₂]

Table S7 Bond lengths [\AA] in compounds **1b–4d**.

1b	
Bi(1)–Br(5)	2.7373(13)
Bi(1)–Br(4)	2.7463(14)
Bi(1)–I(6)	2.807(11)
Bi(1)–Br(6)	2.842(10)
Bi(1)–Br(1)	3.1003(13)
Bi(1)–Br(2)	3.1331(13)
Bi(1)–Br(3)	3.1847(11)
Bi(2)–Br(9)	2.686(12)
Bi(2)–Br(8)	2.742(9)
Bi(2)–Br(7)	2.7719(14)
Bi(2)–I(8)	2.809(16)
Bi(2)–I(9)	2.872(13)
Bi(2)–Br(1)	3.0979(14)
Bi(2)–Br(2)	3.1632(12)
Bi(2)–Br(3)	3.2300(12)
Bi(3)–Br(13)	2.7482(14)
Bi(3)–Br(15)	2.761(7)
Bi(3)–I(14)	2.796(12)
Bi(3)–Br(14)	2.824(7)
Bi(3)–Br(10)	2.9565(15)
Bi(3)–I(15)	3.01(2)
Bi(3)–Br(11)	3.056(4)
Bi(3)–Br(12)	3.062(10)
Bi(3)–I(11)	3.14(3)
Bi(3)–I(12)	3.155(14)
Bi(4)–Br(16)	2.7244(14)
Bi(4)–Br(18)	2.732(15)
Bi(4)–Br(17)	2.7677(15)
Bi(4)–I(18)	2.983(14)
Bi(4)–Br(10)	3.0150(15)
Bi(4)–I(11)	3.03(3)
Bi(4)–Br(11)	3.076(3)
Bi(4)–Br(12)	3.092(10)
Bi(4)–I(12)	3.288(13)

2b	
Bi(1)–Br(5)	2.771(3)

Bi(1)–I(4)	2.7930(15)
Bi(1)–Br(6)	2.834(19)
Bi(1)–I(5)	2.89(4)
Bi(1)–I(6)	2.931(14)
Bi(1)–I(1)	2.9904(15)
Bi(1)–Br(2)	3.117(14)
Bi(1)–I(2)	3.140(4)
Bi(1)–I(3)	3.1628(12)
Bi(2)–Br(9)	2.770(13)
Bi(2)–I(8)	2.7780(15)
Bi(2)–I(7)	2.78(2)
Bi(2)–Br(7)	2.811(9)
Bi(2)–I(9)	2.939(9)
Bi(2)–I(1)	3.0263(15)
Bi(2)–I(3)	3.1125(13)
Bi(2)–Br(2)	3.153(16)
Bi(2)–I(2)	3.242(6)

3b

Bi(1)–I(4)	2.7400(7)
Bi(1)–I(5)	2.746(18)
Bi(1)–Br(5)	2.754(9)
Bi(1)–I(6)	2.755(6)
Bi(1)–Br(6)	2.7576(14)
Bi(1)–I(2)	2.91(2)
Bi(1)–Br(2)	3.082(7)
Bi(1)–Br(3)	3.101(7)
Bi(1)–Br(1)	3.171(12)
Bi(1)–I(1)	3.191(5)
Bi(1)–I(3)	3.305(19)
Bi(2)–I(8)	2.698(17)
Bi(2)–Br(7)	2.749(5)
Bi(2)–I(9)	2.7644(8)
Bi(2)–I(7)	2.810(11)
Bi(2)–Br(8)	2.845(9)
Bi(2)–Br(3)	2.987(6)
Bi(2)–I(2)	3.00(3)
Bi(2)–Br(2)	3.059(9)
Bi(2)–Br(1)	3.158(11)

Bi(2)–I(3)	3.241(18)
Bi(2)–I(1)	3.321(5)

4b_100K

Bi(1)–Br(4)	2.725(12)
Bi(1)–I(3)	2.7863(7)
Bi(1)–I(1)	2.9116(7)
Bi(1)–I(4)	2.943(8)
Bi(1)–I(2)	2.9674(7)
Bi(1)–I(5)	3.0007(7)
Bi(1)–Br(5) (–x, –y+2, –z)	3.0074(7)

4b_150K

Bi(1)–I(3)	2.7935(8)
Bi(1)–I(4)	2.8653(8)
Bi(1)–I(1)	2.9205(8)
Bi(1)–I(2)	2.9791(8)
Bi(1)–I(5)	3.0045(9)
Bi(1)–Br(5) (–x, –y+2, –z)	3.0119(9)

3c

Bi(1)–I(3)	2.9212(6)
Bi(1)–I(4)	2.9311(6)
Bi(1)–I(1)	3.0299(5)
Bi(1)–I(2)	3.1666(5)
Bi(1)–I(1) (x, –y+3/2, z–1/2)	3.2782(5)
Bi(1)–I(2) (x, –y+3/2, z+1/2)	3.2834(5)

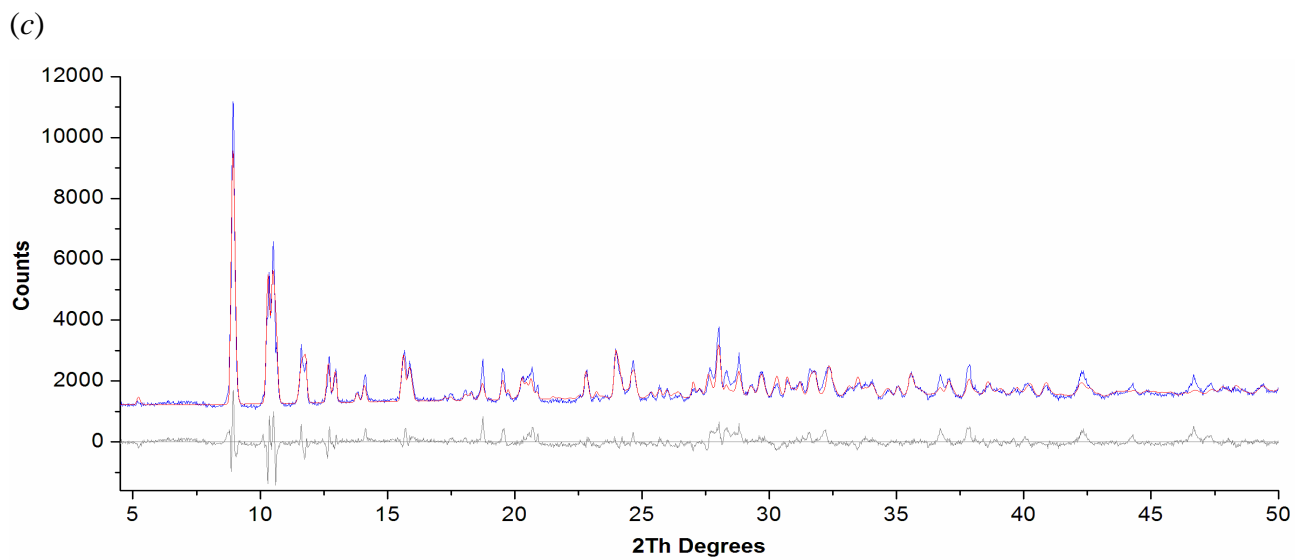
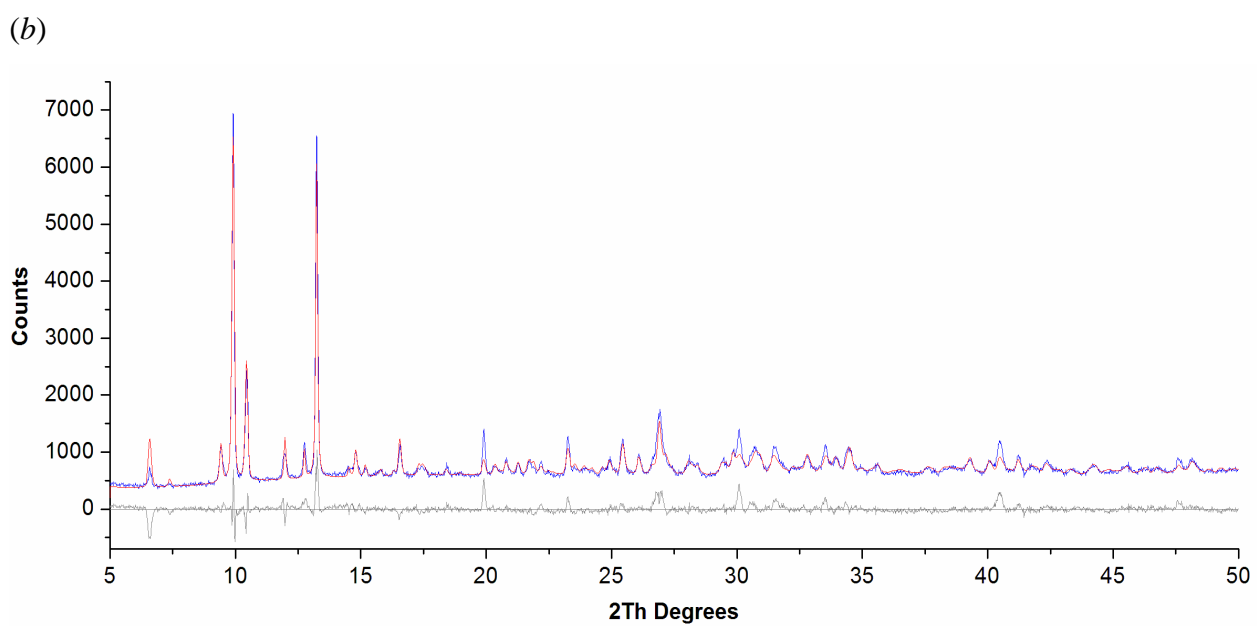
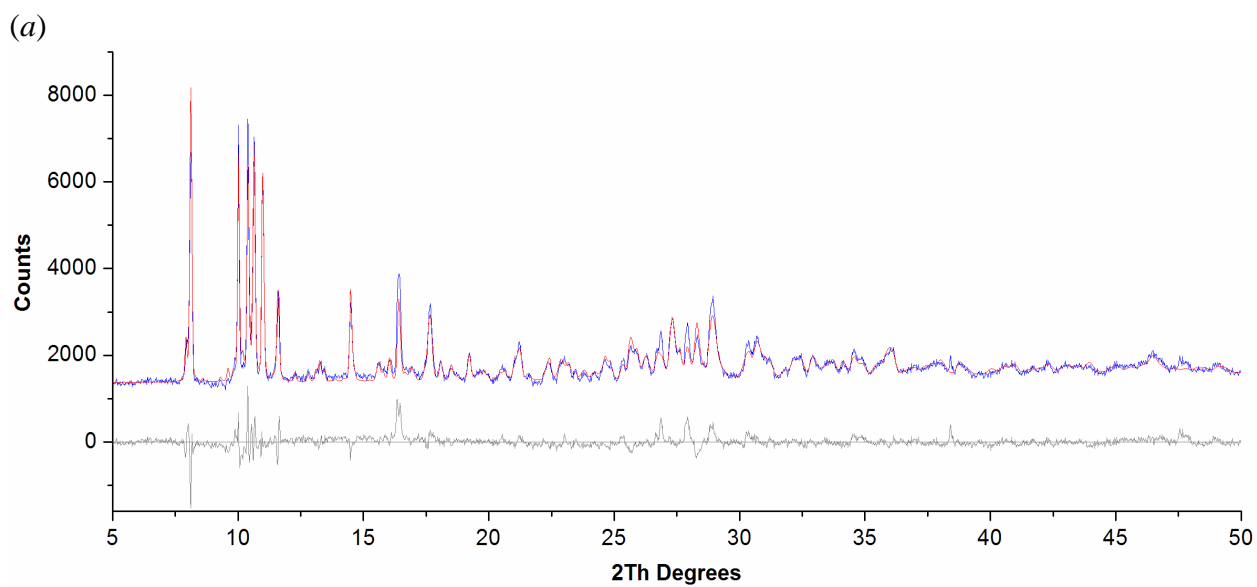
4c

Bi(1)–I(12)	2.818(6)
Bi(1)–I(11)	2.847(3)
Bi(1)–I(13)	2.9721(5)
Bi(2)–Br(22)	2.8791(7)
Bi(2)–Br(21)	2.9077(9)

4d

Bi(1)–I(2)	3.0011(3)
Bi(1)–I(6)	3.0434(4)
Bi(1)–I(4)	3.0444(3)
Bi(1)–I(1)	3.1315(4)

Bi(1)–I(5)	3.1341(3)
Bi(1)–I(3)	3.1901(3)
Bi(1)–K(1)	4.30462(17)
I(1)–K(1)	3.4477(3)
I(3)–K(1)	3.4985(3)
I(5)–K(1)	3.5914(3)



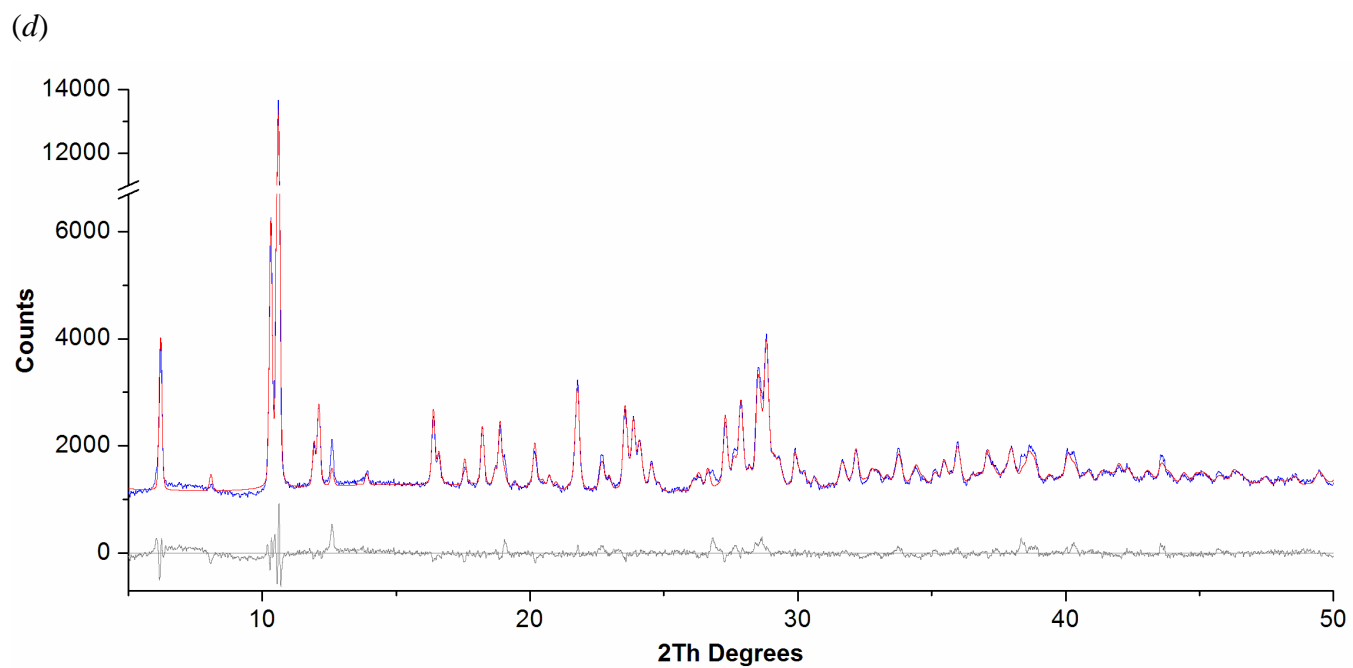


Figure S1 X-ray Rietveld refinement profiles for compounds (a) **1b**, (b) **2b**, (c) **3b**, and (d) **4b** recorded at RT. Red and blue lines correspond to the calculated profile and experimental pattern, respectively. The bottom trace shows the difference curve.

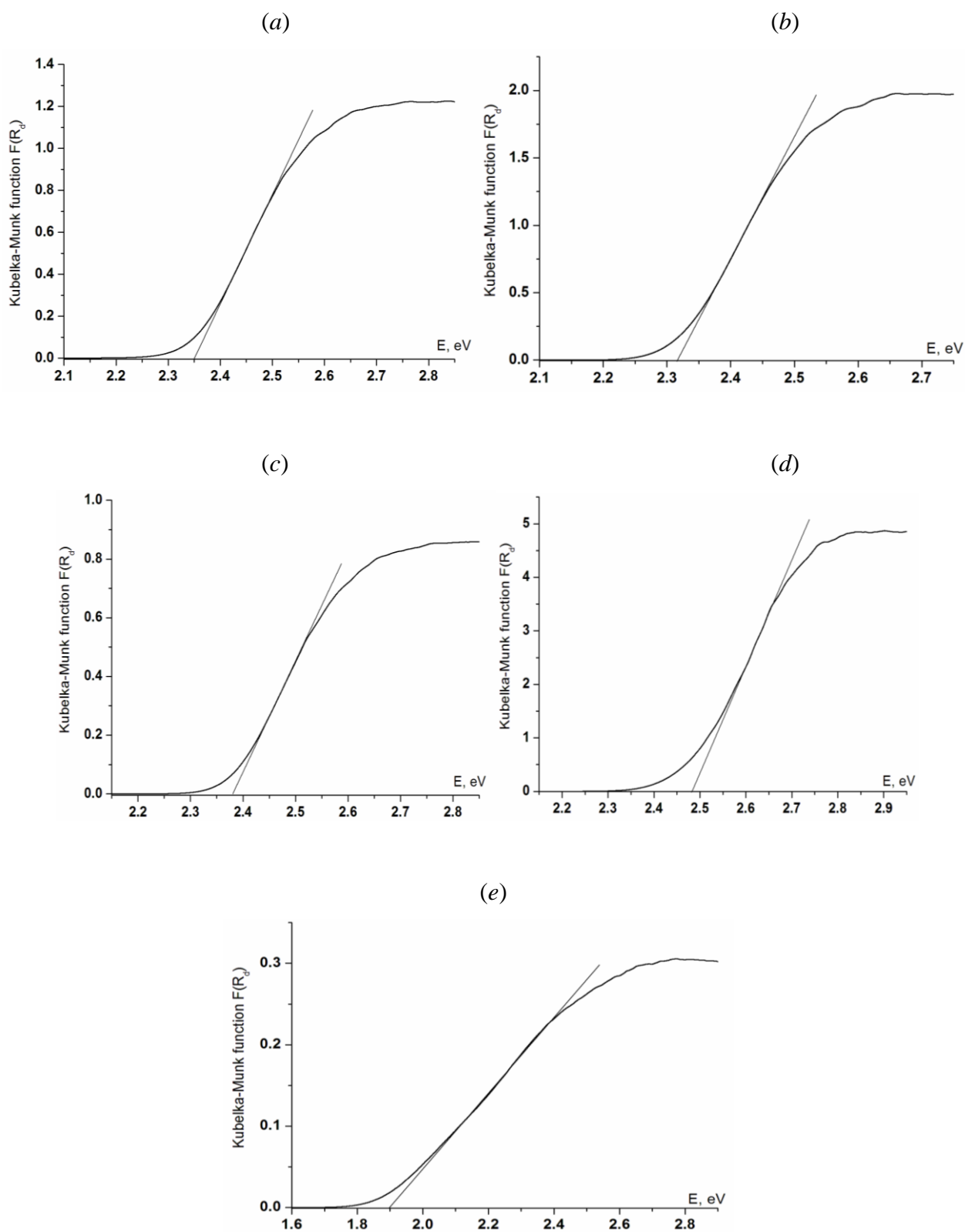
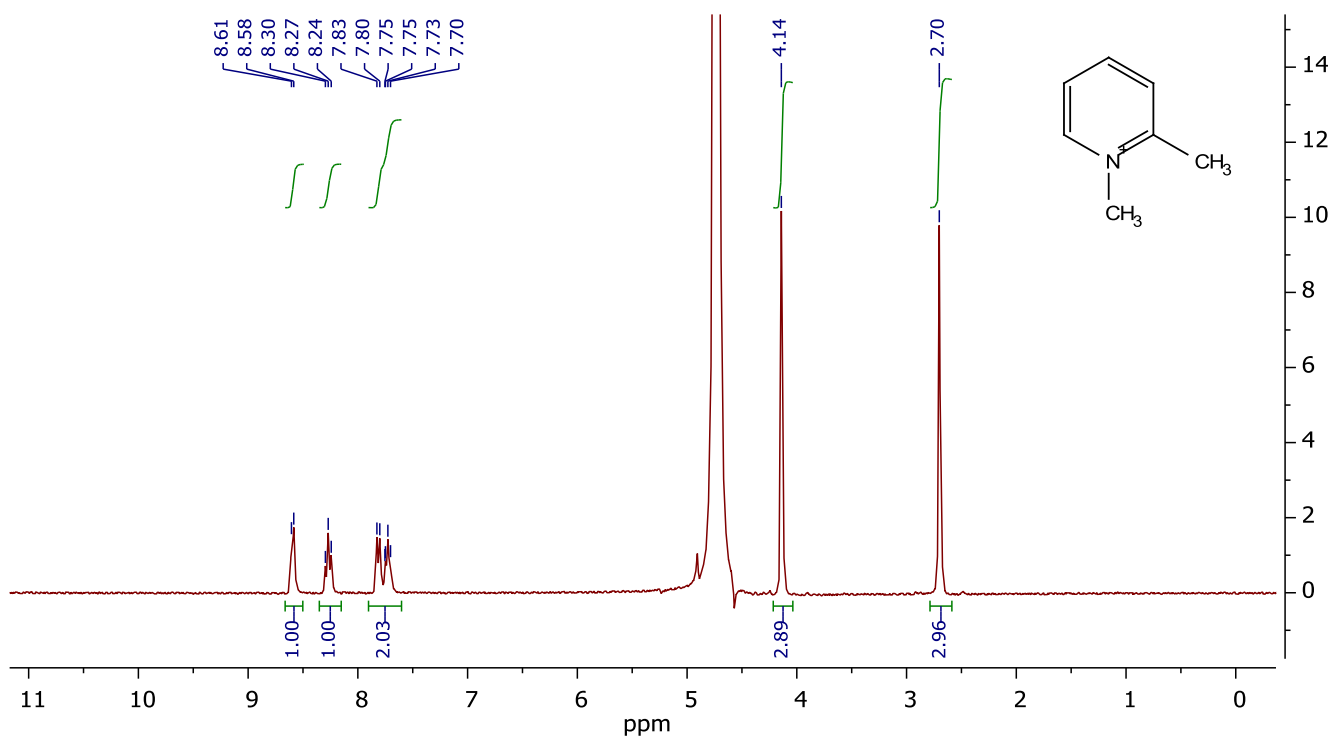


Figure S2 The reflectance spectra of compounds (a) **1b**, (b) **2b**, (c) **3b**, (d) **4b**, and (e) **4c**.

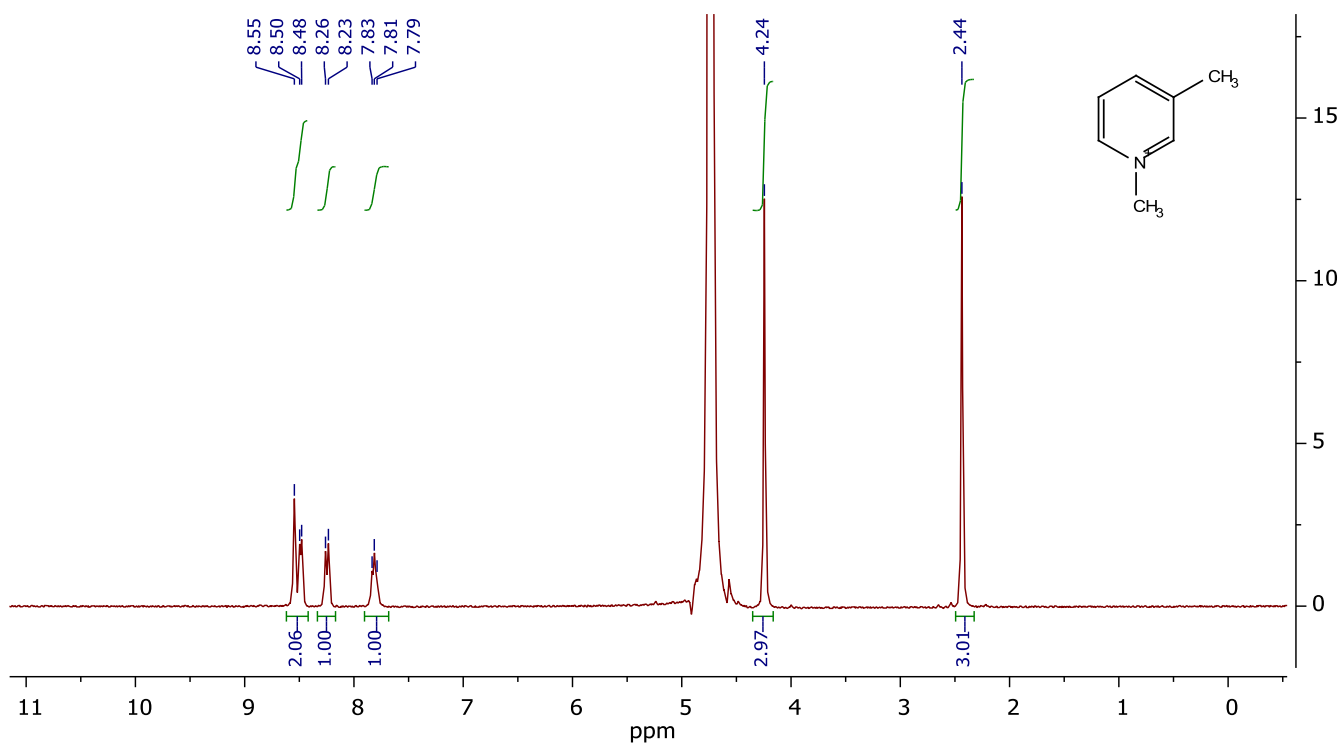
The ^1H NMR spectra were recorded using a Bruker AVANCE 300 instrument operating at 300 MHz frequency at 303 K.

The ^1H NMR spectra were recorded using a Bruker AVANCE 300 instrument operating at 300 MHz frequency at 303 K.

(a)



(b)



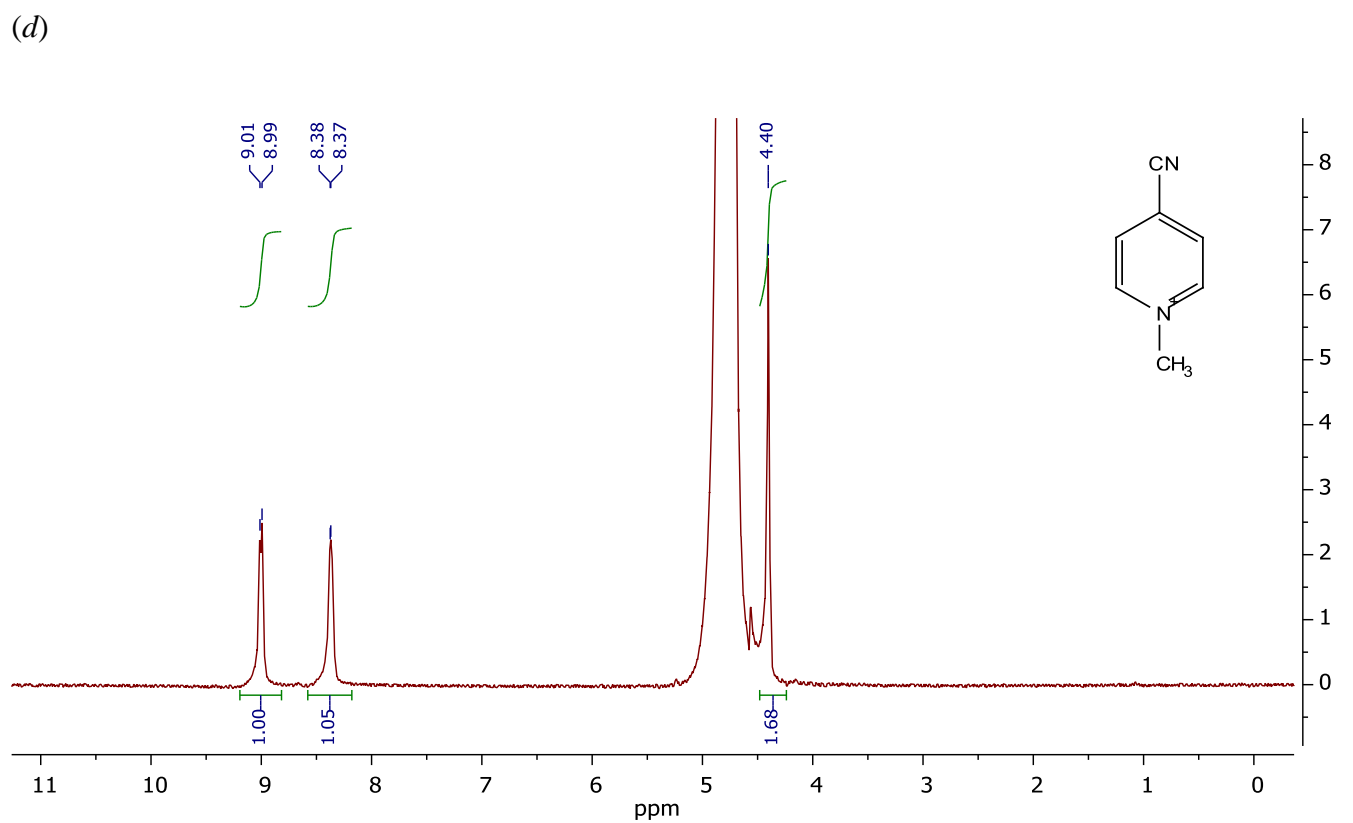
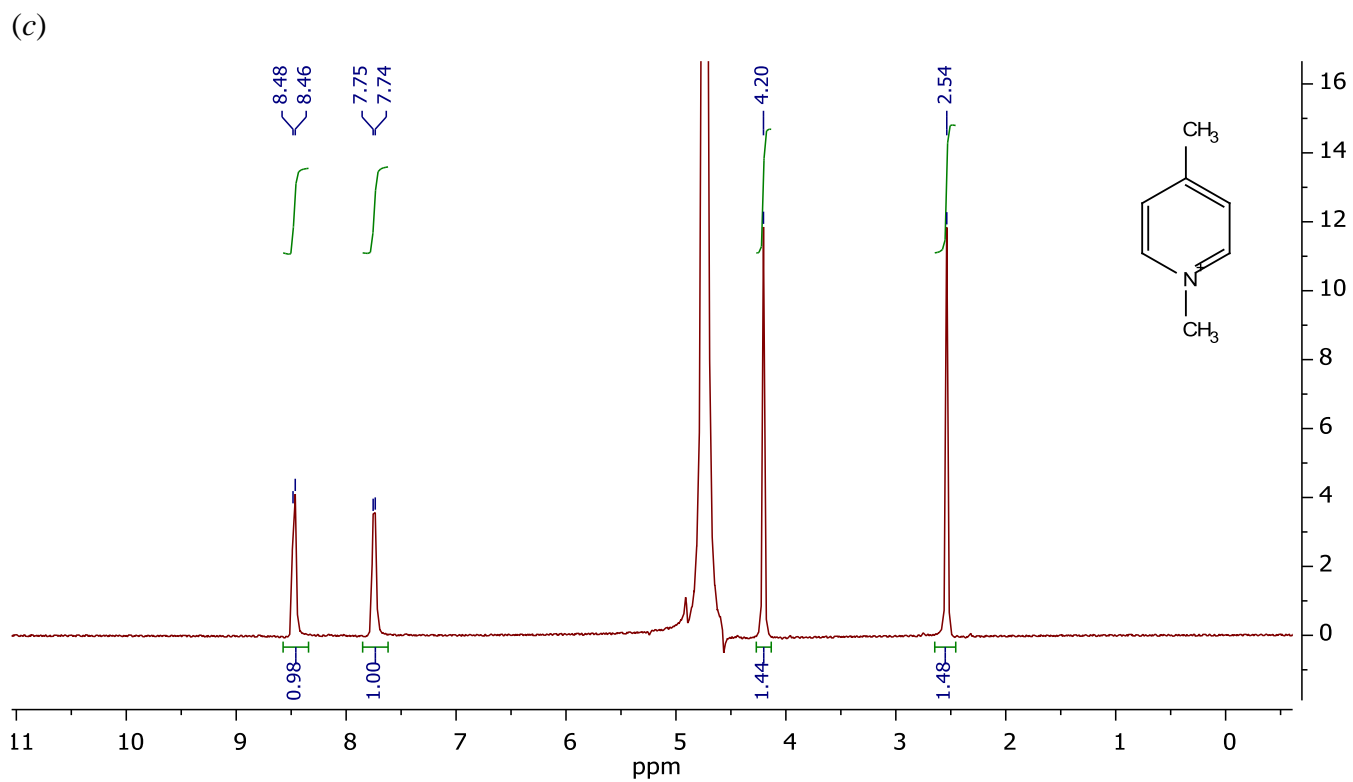
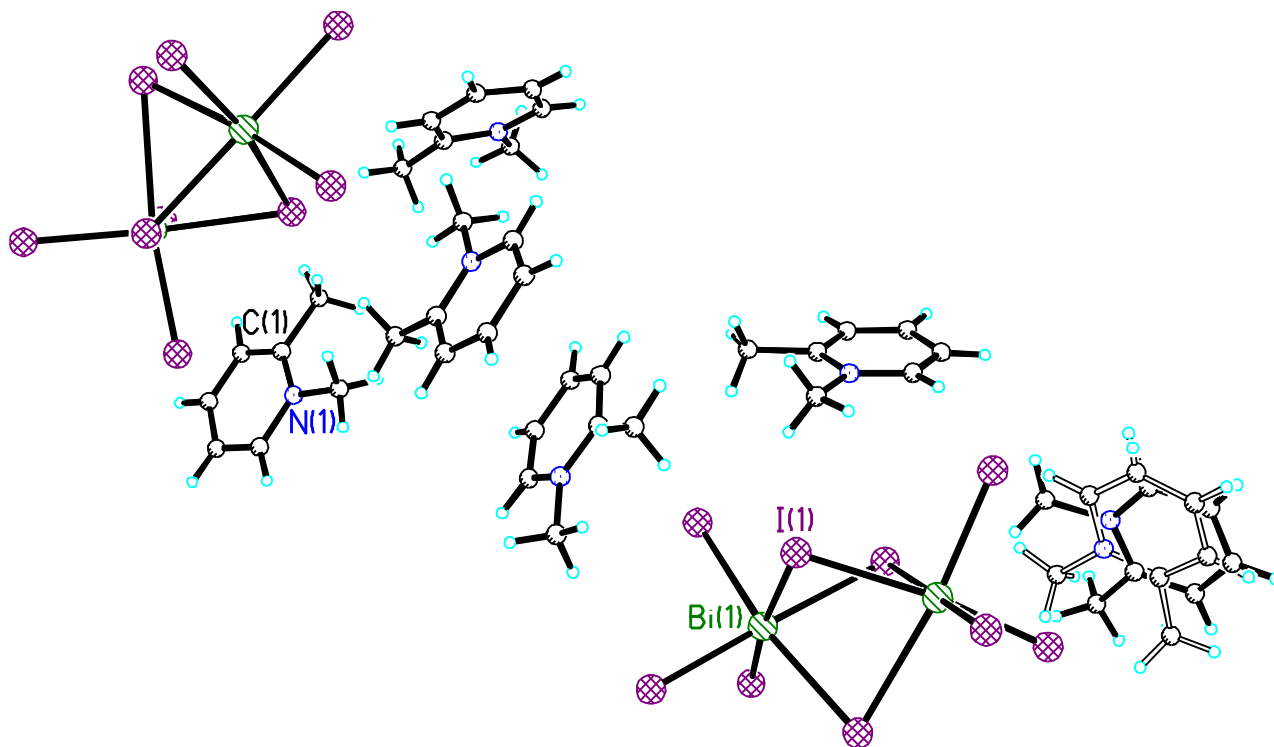


Figure S3 ^1H NMR spectra of compounds (a) **1a**, (b) **2a**, (c) **3a**, and (d) **4a**.

(a)



(b)

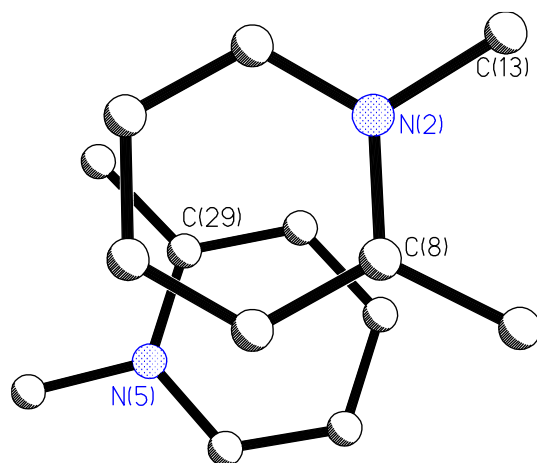
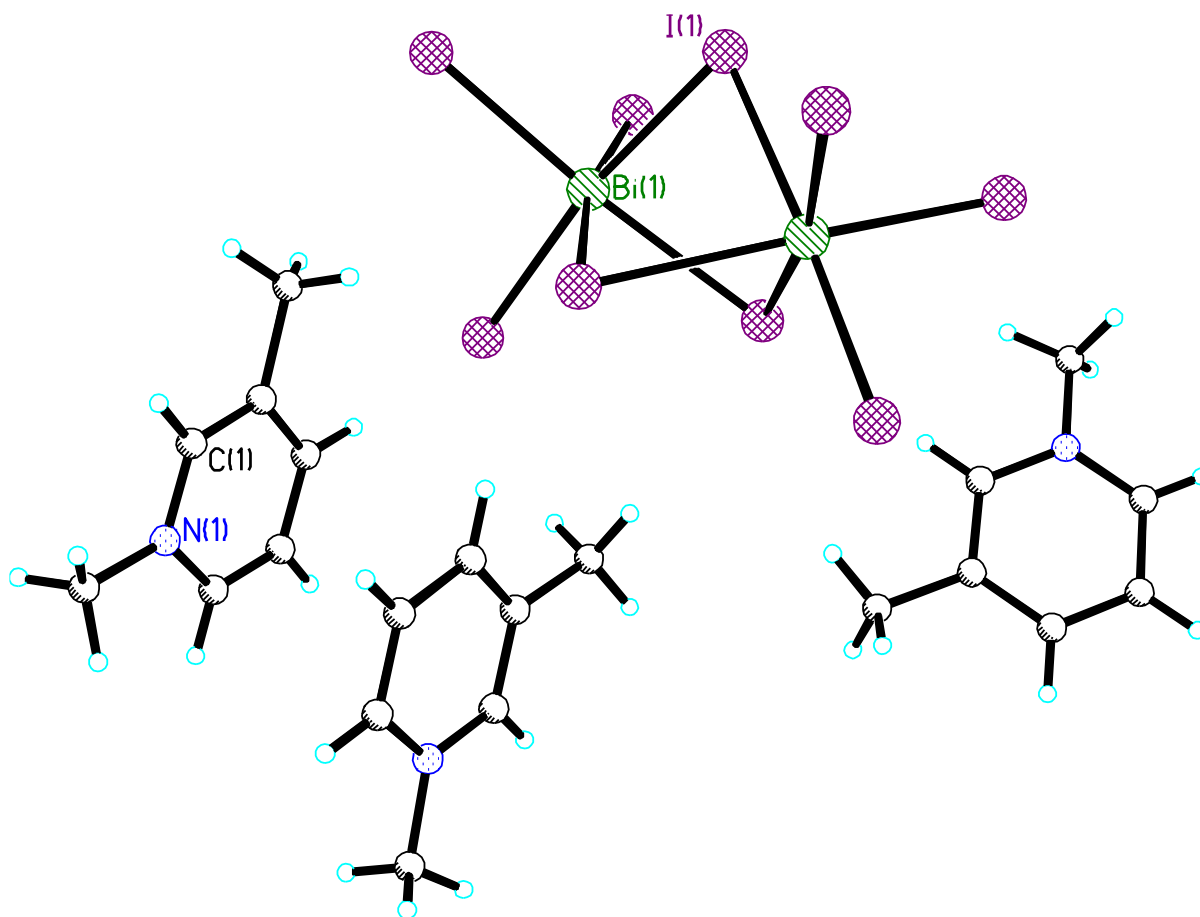
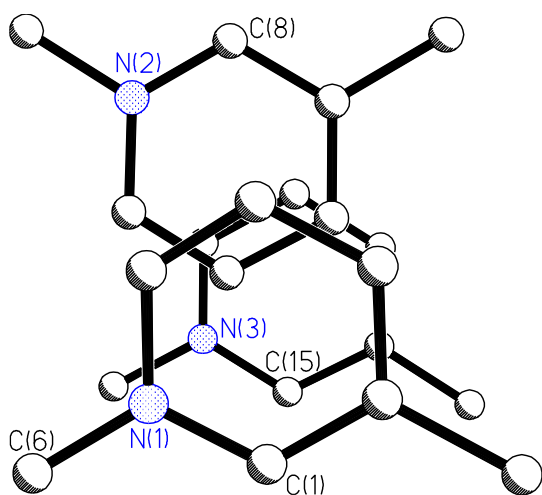


Figure S4 (a) A fragment of structure of $[1,2\text{-Me}_2\text{Py}]_6[\text{Bi}_2\text{Br}_6\text{I}_3][\text{Bi}_2\text{Br}_{6.85}\text{I}_{2.15}]$ (**1b**), where the Br atoms are omitted for clarity; and (b) stacking interaction between two cations.

(a)



(b)



(c)

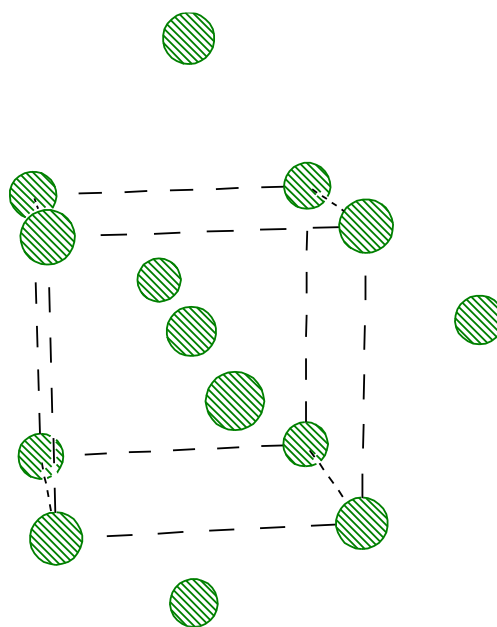
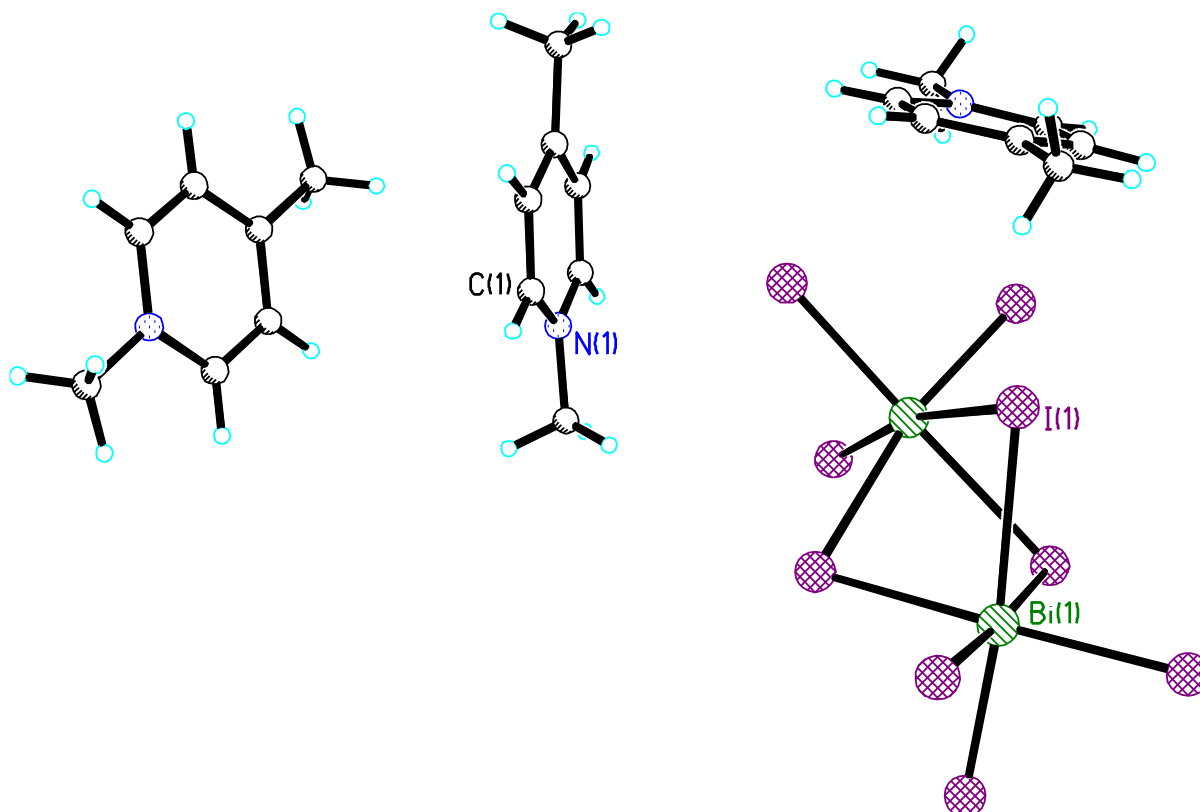


Figure S5 (a) A fragment of structure of $[1,3\text{-Me}_2\text{Py}]_3[\text{Bi}_2\text{Br}_{6.26}\text{I}_{2.74}]$ (**2b**), where the Br atoms are omitted for clarity; (b) the stacking interaction between cations and mutual arrangement of anions; and (c) the Bi–Bi segment centers in one anion.

(a)



(b)

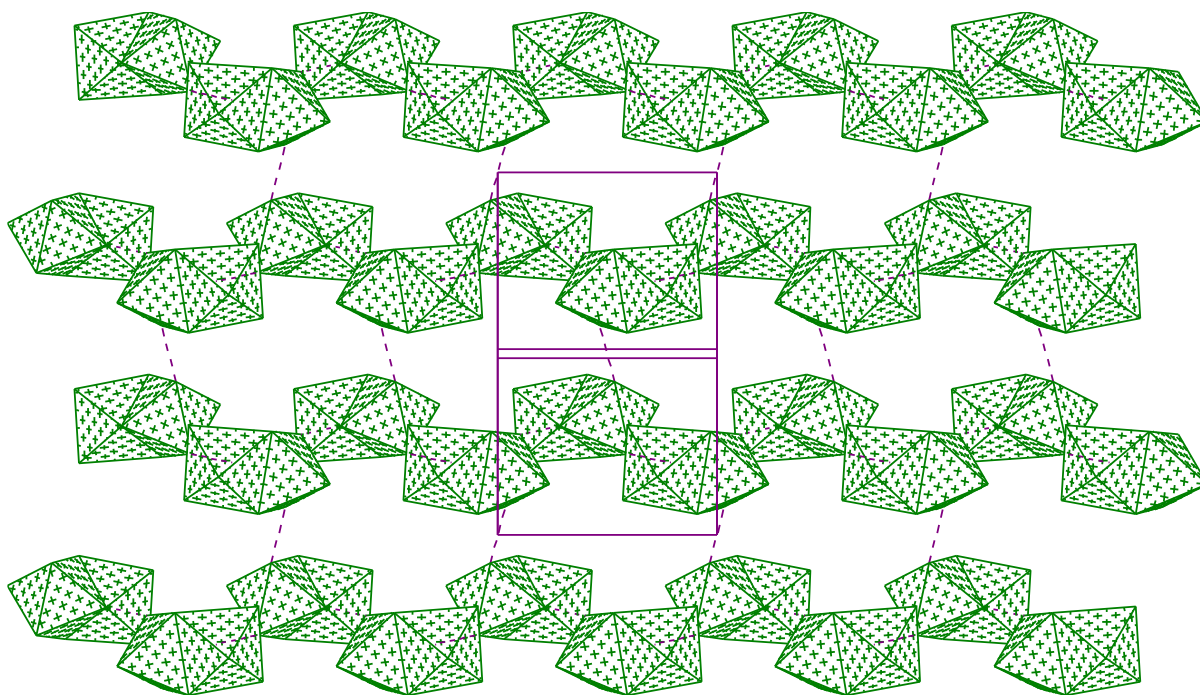
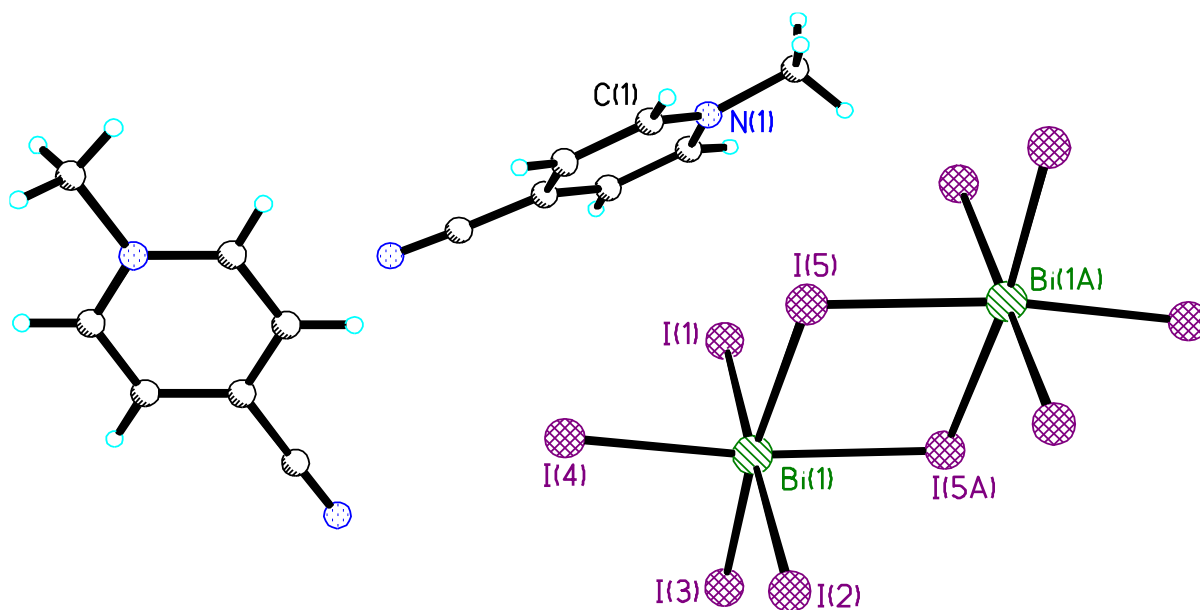


Figure S6 (a) A fragment of the structure of $[1,4\text{-Me}_2\text{Py}]_3[\text{Bi}_2\text{Br}_{6.60}\text{I}_{2.40}]$ (**3b**), where the Br atoms are omitted for clarity; and (b) the structure of anion layer.

(a)



(b)

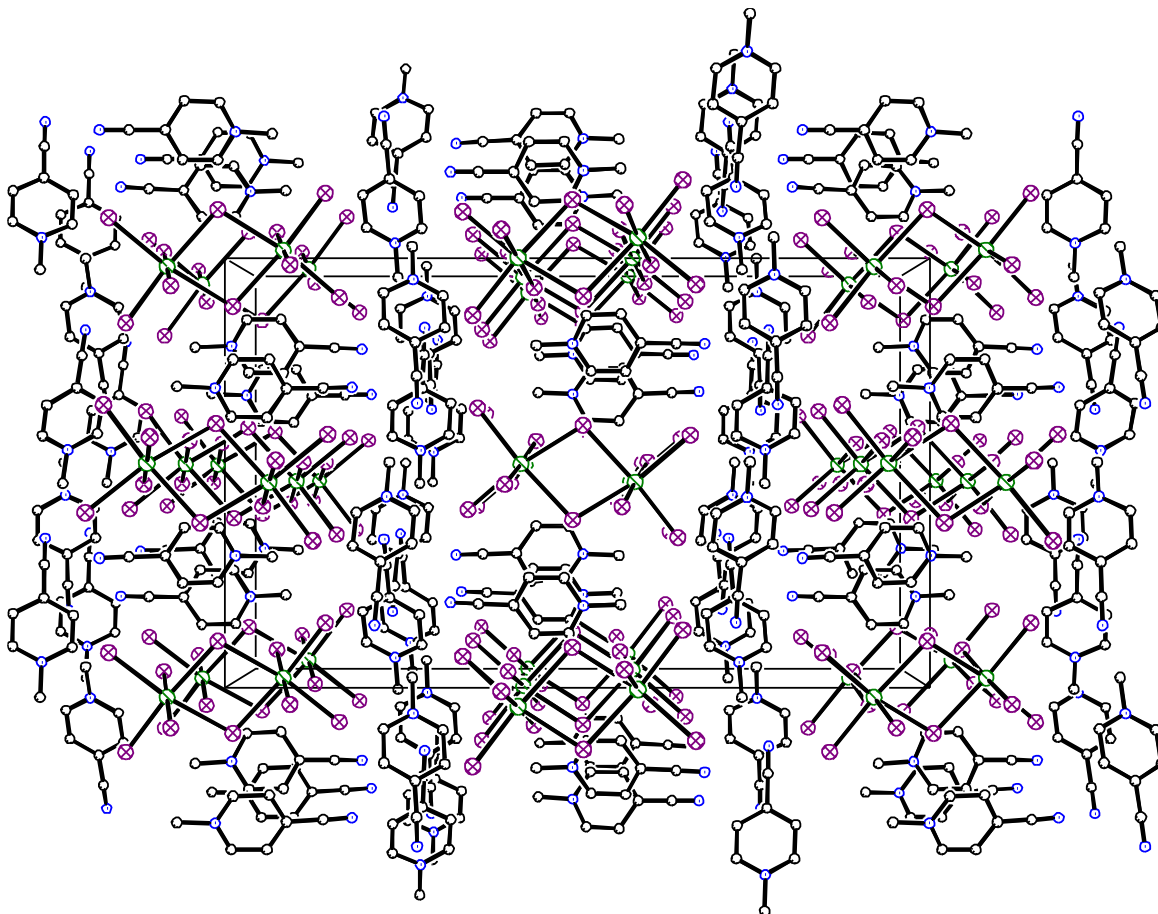
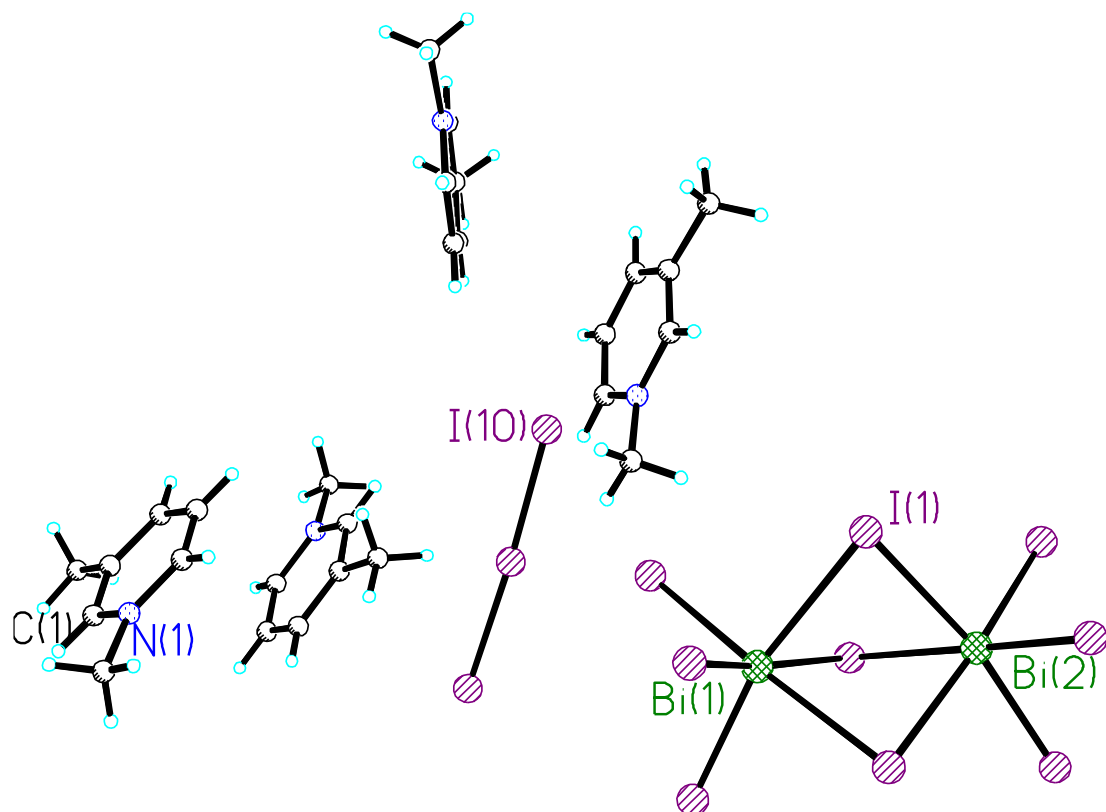


Figure S7 (a) A fragment of the structure of $[4\text{-CNMePy}]_4[\text{Bi}_2\text{Br}_{7.42}\text{I}_{2.58}]$ (**4b_100K**), where the Br atoms are omitted for clarity; and (b) the projection along axis y .

(a)



(b)

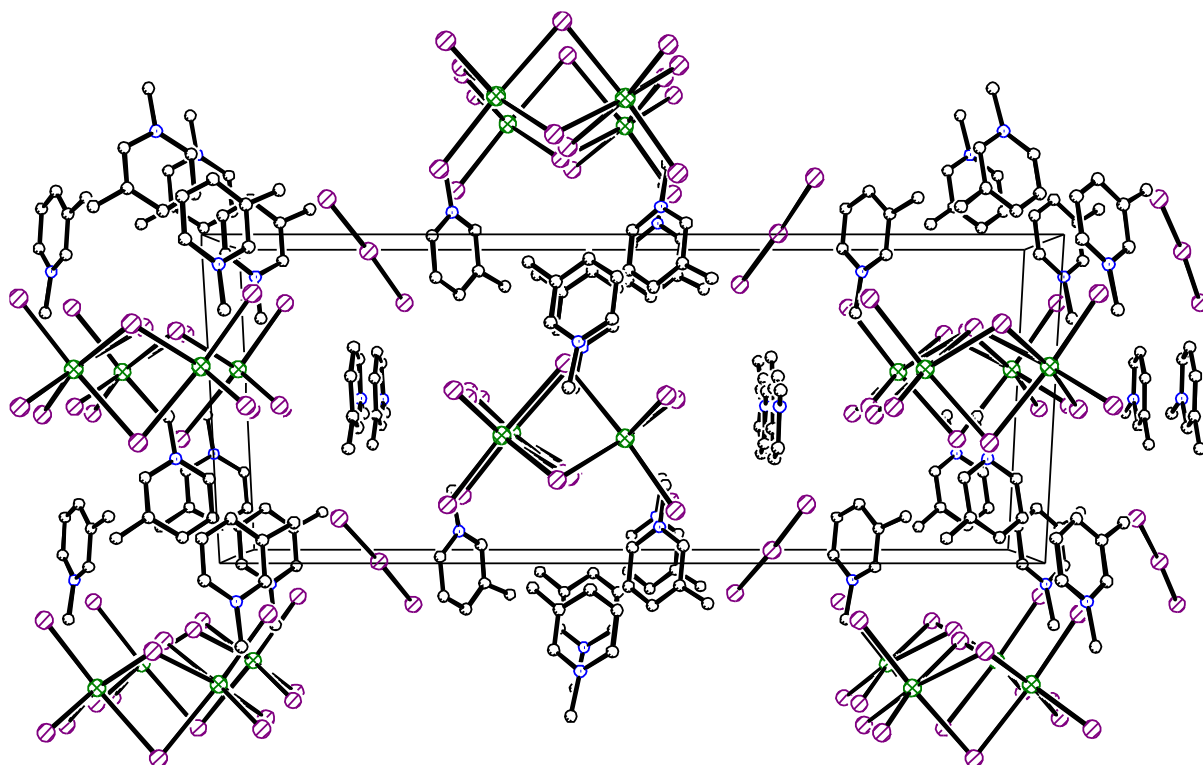


Figure S8 (a) A fragment of the structure of [1,3-Me₂Py]₄[Bi₂I₉]I₃ (**2c**) and (b) the projection along axis *x*.

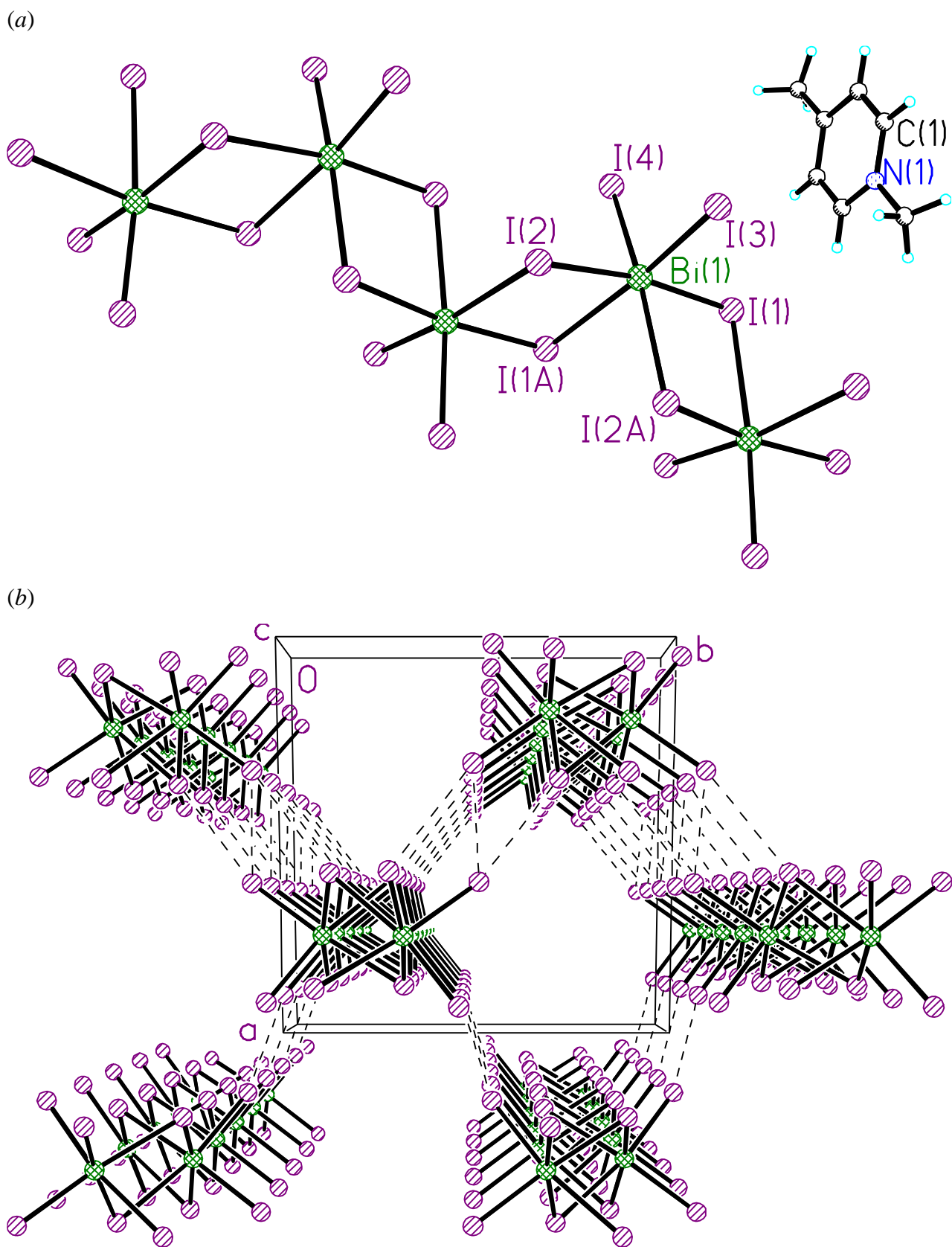


Figure S9 (a) A fragment of the structure of [1,4-Me₂Py][BiI₄] (**3c**) and (b) a projection of the anion sublattice along axis *z*.

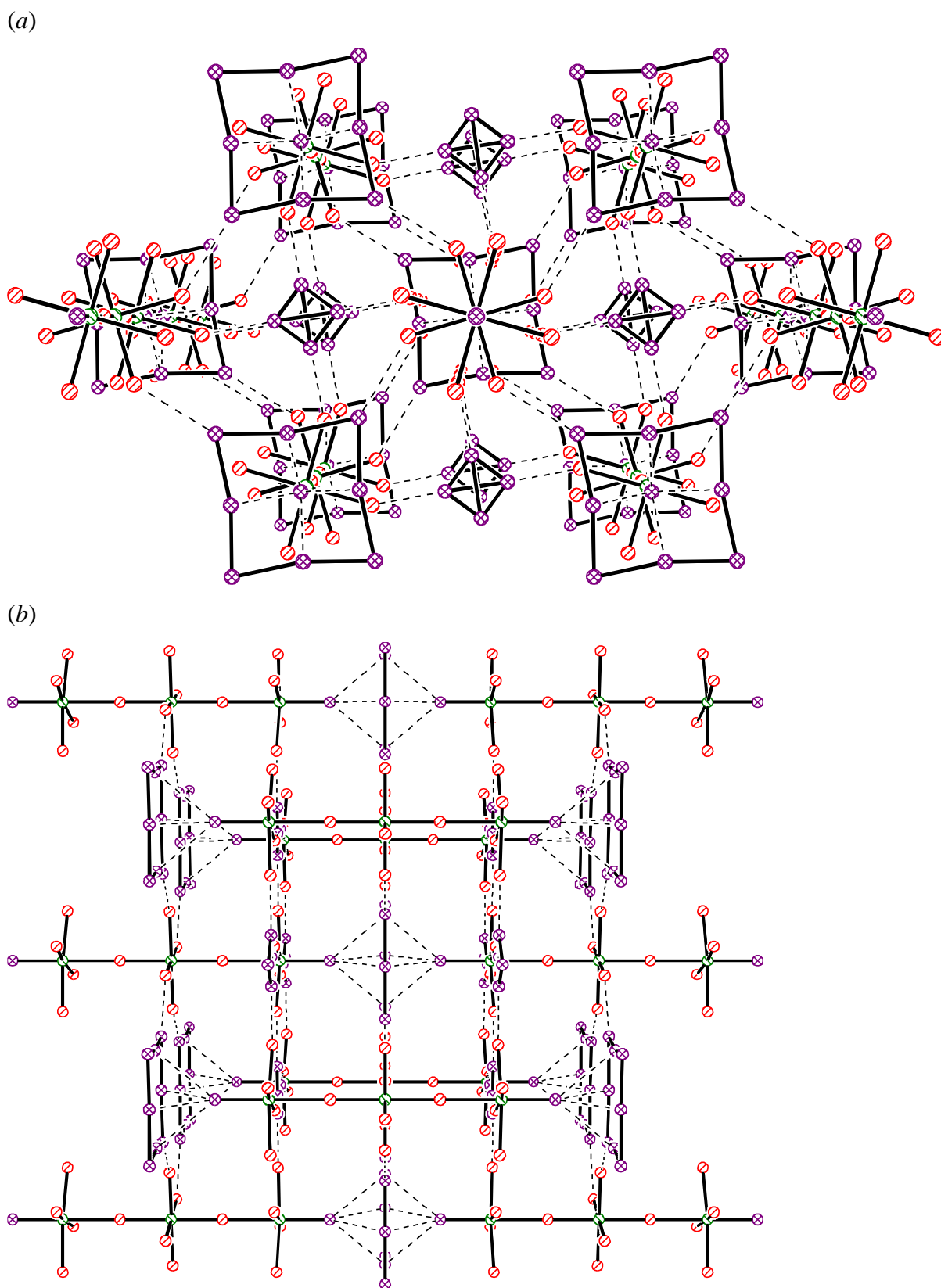


Figure S10 Projection of the anion sublattice (+ I₂ molecules) in the structure of [4-CNMePy]₈[Bi₃Br₁₂I₄]I₇·2(I₂) (**4c**) along axes (a) *z* and (b) *x*. The I₂ molecule is shown as a small square with diagonals, while the I₇⁻ anion is shown as a large square.

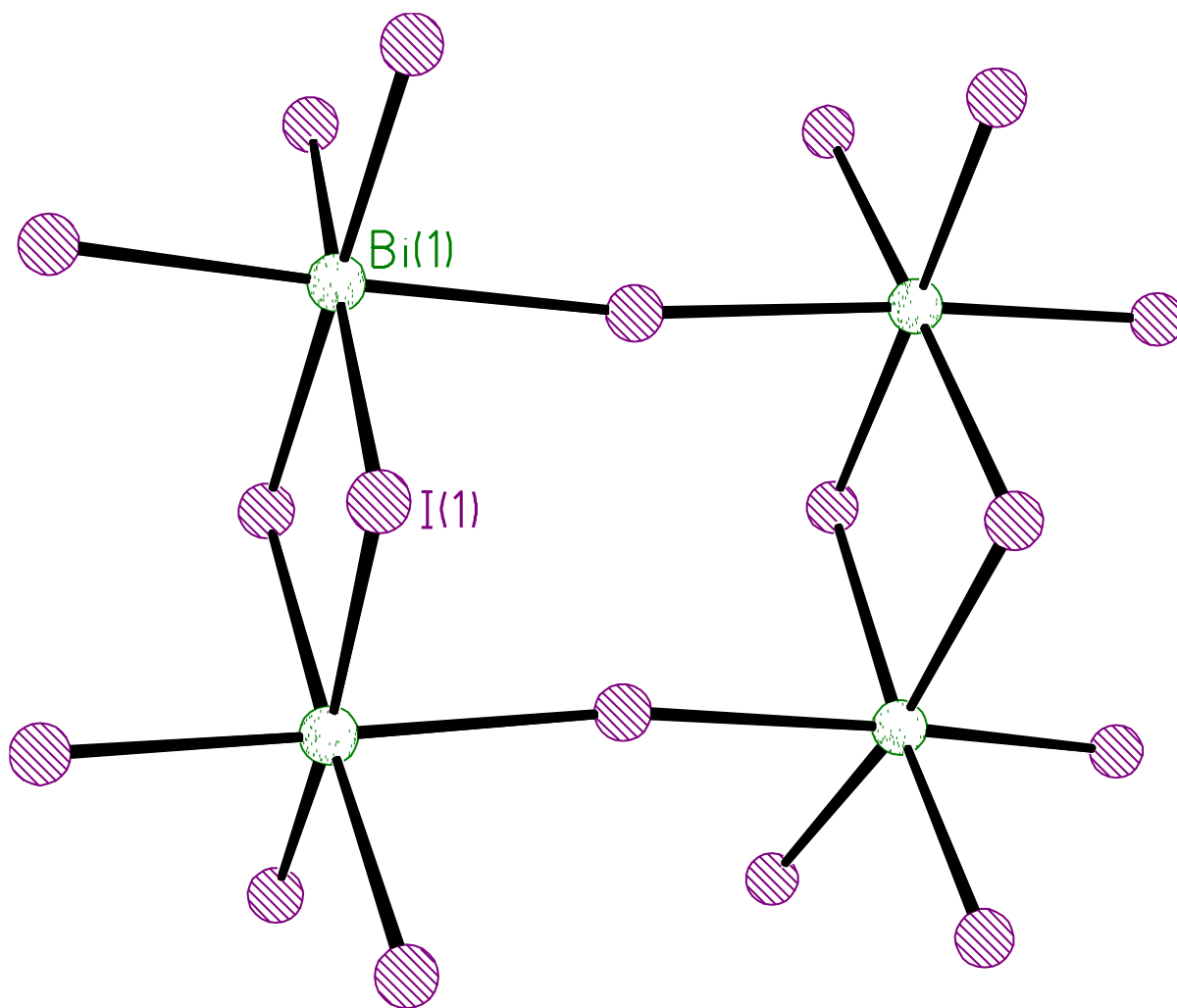


Figure S11 The structure of tetranuclear anion $[\text{Bi}_4\text{I}_{18}]^{6-}$ in the structure of $\text{K}_{5.64}(\text{H}_3\text{O})_{4.36}[\text{4-CNMePy}]_8[\text{Bi}_4\text{I}_{18}]_3 \cdot 4.13\text{H}_2\text{O}$ (**4e**).

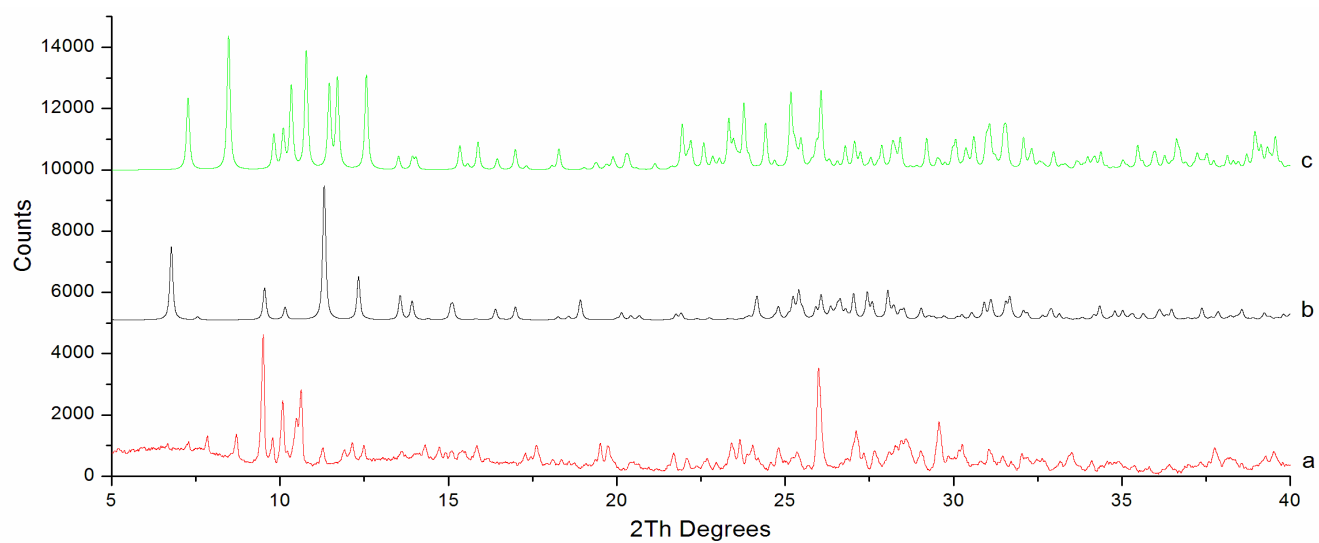


Figure S12 XRD patterns of (a) **4f** (experimental pattern), (b) **4e** (calculated profile), and (c) **4d** (calculated profile).